[Neutrosophic Sets and Systems](https://digitalrepository.unm.edu/nss_journal)

Volume 55 Article 7

5-1-2023

Expression and Analysis of Scale Effect and Anisotropy of Joint Roughness Coefficient Values Using Confidence Neutrosophic Number Cubic Values

Zhenhan Zhang

Jun Ye

Neutrosophic Sets and Systems, Vol. 55, 2023
University of New Mexico

Expression and Analysis of Scale Effect and Anisotropy of Joint Roughness Coefficient Values Using Confidence Neutrosophic Number Cubic Values

Zhenhan Zhang, Jun Ye *

School of Civil and Environmental Engineering, Ningbo University, Ningbo 315211, P.R. China
E-mail: zhangzhenhan97@gmail.com, yejun1@nbu.edu.cn

* Correspondence: yejun1@nbu.edu.cn

Abstract: The JRC data collected from a rock mass joint surface difficultly obtain enough large-scale JRC sample data, but small-scale JRC sample data, which usually contain indeterminate and incomplete information due to the limitation of the measurement environment, measurement technology, and other factors. In this case, the existing representation and analysis methods of the JRC sample data almost all lack the measures of confidence levels in the sample data analysis. In this paper, we propose the concept and expression method of confidence neutrosophic number cubic values (CNNCVs), and then establish CNNCVs of joint roughness coefficient (JRC) (JRC-CNNCVs) from the limited/small-scale JRC sample data subject to the normal distribution and confidence level of the JRC sample data to analyze the scale effect and anisotropy of JRC values. In the analysis process, the JRC-CNNCVs are first conversed from the JRC sample data (multi-valued sets) in view of their distribution characteristics and confidence level. Next, JRC-CNNCVs are applied to analyze the scale effect and anisotropy of the JRC values by an actual case, and then the effectiveness and rationality of the proposed expression and analysis method using JRC-CNNCVs are proved by the actual case in a JRC multi-valued environment. From a perspective of probabilistic estimation, the established expression and analysis method makes the JRC expression and analysis more reasonable and reliable under the condition of small-scale sample data.

Keywords: confidence neutrosophic number; confidence neutrosophic number cubic value; joint roughness coefficient; scale effect; anisotropy

1. Introduction

Joint roughness coefficient (JRC) was first proposed by Barton [1] and estimated through experience. Then, JRC is a key index that affects the shear strength of the rock joint. To make the JRC value more reasonable and accurate, researchers have proposed many calculation and expression methods of the JRC value, such as statistical parameter methods [2, 3], straight edge methods [4–7], fractal dimension methods [8–11], etc. However, the indeterminate and incomplete information contained in the JRC values is not considered in the above studies. Due to the irregularity of the rock mass joint surface, the JRC values at different positions on the same joint are different, which also means that the JRC values imply some uncertainty. Numerous studies have shown that the JRC values reflect their scale effect [12–15] and decrease with increasing sample scale. Another obvious characteristic of the JRC values is anisotropy [16–19], that is, the JRC values in different measurement directions of the same rock mass joint is different. Both of these characteristics reflect incomplete and indeterminate information contained in the JRC values. Furthermore, some studies [20, 21] have shown that sampling bias is also an important factor causing the indeterminacy of JRC values.

As an important branch of neutrosophic theory, a neutrosophic number (NN) was first proposed by Smarandache [22–24] from the perspective of the symbol. Then, Ye [25–27] gave the calculation rules of NNs from the perspective of the numerical value and generalized their application in practical problems. Subsequently, related theories of NN have been applied to the decision making/evaluation of investment projects, manufacturing schemes, software testing, goal programming, air quality, etc. [28–33]. NN can generally be expressed as $E(I) = v + \eta I$, where v is the determinate part and ηI is the indeterminate part, the indeterminacy $I \in [I^L, I^U]$, and $v, \eta \in R$ (all real numbers). According to an indeterminate range of $I \in [I^L, I^U]$, NN can represent all values in an interval. Therefore, it is very suitable for the expression of the JRC value because NN can express incomplete and indeterminate information flexibly and conveniently. Yong et al. [34] applied NN to the expression of the JRC value and utilized the NN function to analyze the anisotropy and scale effect of the JRC values. Although this research effectively considers the uncertainty in the JRC values, this method requires the use of a fitting function, where may loss some useful information in the fitting process. To avoid this defect, some scholars combined the theory of neutrosophic statistics with NN to express the JRC values by JRC-NNs [35–37]. Furthermore, Chen et al. [38] combined neutrosophic probability with NN and proposed neutrosophic interval probability (NIP) and neutrosophic interval statistical number (NISN) to express JRC values. Although this method makes the JRC-NN/interval value confident to a certain degree, this method still lacks some probabilistic estimation since the confidence level/interval of the neutrosophic probabilities (P_T, P_I, P_F) is not considered in NIP. It is difficult to ensure the probabilistic credibility of the JRC values within the NIP obtained from the limited JRC sample data. Then, Zhang and Ye [39] presented (fuzzy) confidence neutrosophic number cubic sets (CNNCSs) in a fuzzy multi-valued setting and used them for group decision-making problems with fuzzy multi-valued sets. Motivated by the notion of the fuzzy CNNCS, this paper introduces a confidence NN cubic value (CNNCV) in light of the probability distribution and confidence level of multi-valued sets. Then, considering the probability distribution and confidence level of the JRC values in the actual environment of small-scale JRC sample data, we convert the JRC multi-valued sets obtained from the rock mass in Changshan County (Zhejiang Province, China) into JRC-CNNCVs as the mixed representation form of the JRC confidence intervals and the JRC average values. The proposed expression method of JRC-CNNCVs can ensure that the JRC values fall within confidence neutrosophic numbers (CNNs) (confidence intervals with some confidence level of (1–α)%) from a probabilistic point of view and reveal the magnitude of the JRC mean. Finally, the scale effect and anisotropy of the JRC values are analyzed by JRC-CNNCVs to verify the validity and rationality of the proposed expression and analysis method in the actual environment of the limited/small-scale JRC sample data. Under the condition of small-scale JRC sample data, the expression and analysis method proposed in this study reflects the obvious advantage, as it is more suitable for engineering applications.

The rest of this paper is organized as follows. Section 2 gives the definition of CNNCV in view of the fuzzy CNNCS. Section 3 converts the actual measured JRC multi-valued sets into JRC-CNNCVs in terms of the normal distribution and confidence level of the JRC values, and then analyzes the scale effect and anisotropy of the JRC values by JRC-CNNCVs. Finally, conclusions and further research are given in Section 4.

2. CNNCVs

In this section, we give the definition of CNNCV in terms of the normal distribution of a multi-valued set and the confidence level of (1–α)% for a level α as an extension of the fuzzy CNNCS.

First, we introduce the notions of NN [22–24], NN probability [40], and CNN [39, 40]. The NN $E(I) = v + \eta I$ consists of two parts, including the determinate part ω and the indeterminate part ηI subject to the indeterminacy $I \in [I^L, I^U]$ and $v, \eta \in R$. Obviously, NN (changeable interval number for

$I \in [I^L, I^U]$) can conveniently express both the determinate information and the indeterminate information contained in the indeterminate situation by $E(I) = [v + \eta I^L, v + \eta I^U]$. Especially when considering $E(I)$ as the value of a random variable t in $[v + \eta I^L, v + \eta I^U]$ with the distribution function $p(t)$ (e.g., normal distribution function), the definition of NN probability is introduced as follows [40]:

$$P(t) = p(v + \eta I^L \le t \le v + \eta I^U) = \int_{v+\eta I^L}^{v+\eta I^U} p(t)dt \ . \tag{1}$$

The larger the NN probability for the variable t, the larger the range of indeterminacy I, that is, the larger the indeterminate interval.

Assuming that there is a multi-valued set $X = \{x_1, x_2, \ldots, x_n\}$ and x_i ($i = 1, 2, \ldots, n$) in X obeys the normal distribution, then the average value v and the standard deviation k of the data in X are given as follows:

$$v = \frac{1}{n}\sum_{i=1}^{n} x_i \ , \tag{2}$$

$$k = \sqrt{\frac{1}{n-1}\sum_{i=1}^{n}(x_i - v)^2} \ . \tag{3}$$

Thus, the multi-valued set X with a confidence level of $(1-\alpha)\%$ can be converted into the CNNCV $E_X(I_\alpha)$ by the following equation:

$$E_X(I_\alpha) = \left\langle [E^L(I_\alpha), E^U(I_\alpha)], v \right\rangle = \left\langle \left[v + \eta I^L, v + \eta I^U \right], v \right\rangle = \left\langle \left[v - \frac{k}{\sqrt{n}} t_{\alpha/2}, v + \frac{k}{\sqrt{n}} t_{\alpha/2} \right], v \right\rangle, \tag{4}$$

where the indeterminate range of I_α is $[I^L, I^U] = [-t_{\alpha/2}, t_{\alpha/2}]$ and $t_{\alpha/2}$ is the critical value that is adopted from [39, 40] in view of confidence levels of $(1-\alpha)\%$ (commonly take $t_{\alpha/2}$ = 1.645, 1.96, 2.576 for the confidence levels of 90%, 95% and 99% [40]).

Example 1. There is a multi-valued set B = {6.32, 1.56, 2.39, 18.35, 10.32, 2.33, 5.77, 3.98, 8.82, 16.32, 9.35, 15.98, 5.58, 11.90, 10.06, 9.33, 5.52, 12.48, 4.46, 10.28} with the normal distribution. Then, the conversing process from the multi-valued set B to the CNNCV E_B is shown below.

First, the mean and standard deviation of the multi-valued set B can be calculated by Eqs. (2) and (3):

(i) $v_B = \frac{1}{n}\sum_{i=1}^{n} b_i = \frac{1}{20}\sum_{i=1}^{20} b_i = 8.56$;

(ii) $k_B = \sqrt{\frac{1}{n-1}\sum_{i=1}^{n}(b_i - v_B)^2} = 4.82$.

Using Eq. (4) with the most common confidence level of 95% and the critical value $t_{\alpha/2}$ = 1.96 [40], the CNNCV E_B corresponding to B can be obtained below:

$$E_B = \left\langle \left[v_B + \eta_B I^L, v_B + \eta_B I^U \right], v_B \right\rangle = \left\langle \left[v_B - \frac{k_B}{\sqrt{n}} t_{\alpha/2}, v_b + \frac{k_B}{\sqrt{n}} t_{\alpha/2} \right], v_B \right\rangle$$

$$= \left\langle \left[8.56 - 1.96 \times 4.82 / \sqrt{20}, 8.56 + 1.96 \times 4.82 / \sqrt{20} \right], 8.56 \right\rangle = \left\langle [6.45, 10.67], 8.56 \right\rangle,$$

where the indeterminate range of I is $[I^L, I^U] = [-t_{\alpha/2}, t_{\alpha/2}] = [-1.96, 1.96]$.

From this example, we get the CNNCV E_B = <[6.45, 10.67], 8.56>, which is composed of the CNN/confidence interval [6.45, 10.67] and the mean 8.56 of B at the confidence level of 95%. Then, we can see that converting the multi-valued set into CNNCV can ensure that 95% probability of the data in B will fall within the CNN/confidence interval [6.45, 10.67], and then 5% probability of the data in B will be outside the CNN/confidence interval [6.45, 10.67], while the mean 8.56 of B reveals the magnitude of the data. Therefore, this conversion approach reflects the advantages of rationality and credibility from the perspective of probabilistic estimation under the condition of small-scale sample data.

3. JRC-CNNCV expression and analysis approach for JRC values

The shear strength of the rock joint surface is recognized as a key parameter in the stability evaluation of engineering rock mass, then JRC is the most important factor affecting the shear strength of the rock mass joint. In practical engineering, the JRC values usually contain a lot of indeterminate and incomplete information, and the measurement of the JRC values is also often limited by the rock joint surface. Therefore, CNNCVs are very suitable for expressing the limited/small-scale JRC sample data.

In this section, we first express the JRC values collected from the rock mass in Changshan County (Zhejiang Province, China) [38] by CNNCVs to give JRC-CNNCVs (including the JRC confidence intervals and the average values). To do so, we introduce the measured data of 240 JRC sample data under 10 sample sizes in 24 measurement directions, and the number of sample data in each multi-valued set is 35. During the measurement process, the measurement directions are divided into 24 directions from 0° to 345° at 15° intervals, and the sample scales are divided into 10 sizes from 10 cm to 100 cm at 10 cm intervals [38]. Then using Eqs. (2) and (3), we calculated the mean v and the standard deviation k of each JRC multi-valued set, which are shown in Table 1.

Many existing studies [41–44] have noted that the distribution of JRC values approximates the normal distribution or left-biased normal distribution after statistical analysis of the JRC values of large-scale sample data. Therefore, in this study, we regard the distribution of the JRC values related to the limited sample data as the normal distribution. In view of the mean and standard deviation of the JRC values, the JRC values (multi-valued sets) are converted into the JRC-CNNCVs at the confidence level of 95% by Eqs. (2)-(4).

Taking the JRC values with the measurement direction of 0° and the sample size of 10 cm as an example, the JRC values are converted into JRC-CNNCV by the following calculation process.

First, it can be seen from Table 1 that the average value v of the JRC values corresponding to the 10 cm sample size in the 0° measurement direction is 10.5861 and the standard deviation k is 2.3026 subject to the 35sample data.

Then using Eq. (4) with the confidence level of 95% and $I_\alpha = [I^L, I^U] = [-1.96, 1.96]$, we can get the following JRC-CNNCV:

$$E_{JRC} = \left\langle [E^L(I_\alpha), E^U(I_\alpha)], v \right\rangle = \left\langle \left[v+\eta I^L, v+\eta I^U \right], v \right\rangle = \left\langle \left[v-\frac{k}{\sqrt{n}} t_{\alpha/2}, v+\frac{k}{\sqrt{n}} t_{\alpha/2} \right], v \right\rangle$$

$$= \left\langle \left[10.5861-1.96\times 2.3026/\sqrt{35}, 10.5861-1.96\times 2.3026/\sqrt{35} \right], 10.5861 \right\rangle = \left\langle [9.8233, 11.3490], 10.5861 \right\rangle.$$

By the similar calculation way, JRC-CNNCVs of E_{JRC} corresponding to the JRC values in other measurement directions and sample sizes are shown in Table 2.

Table 1. The mean v and the standard deviation k of JRC values obtained from 24 different directions under 10 different sample sizes

Direction (°)	Size (cm)	v	k	Direction (°)	Size (cm)	v	k
0	10	10.5861	2.3026	180	10	9.8462	2.1651
	20	9.6833	1.7374		20	9.9489	1.8742
	30	9.3136	1.5113		30	8.7877	1.7512
	40	9.0054	1.7304		40	8.6400	1.6939
	50	8.8621	1.6416		50	8.3278	1.6074
	60	8.8322	1.6281		60	8.1673	1.6464
	70	8.6922	1.6222		70	7.9951	1.5076
	80	8.6070	1.5109		80	7.9080	1.3551
	90	8.5757	1.3621		90	7.8390	1.2001
	100	8.4684	1.2872		100	7.8343	1.0682
15	10	10.7113	2.2212	195	10	9.7585	2.2466

15	20	9.9985	1.7591	195	20	9.2766	1.7717
	30	9.3839	1.6341		30	8.7089	1.7003
	40	9.3013	1.2955		40	8.8393	1.4742
	50	9.2764	1.3036		50	8.5611	1.5763
	60	9.0033	1.3283		60	8.1420	1.5784
	70	8.8430	1.1862		70	7.9523	1.2771
	80	8.5922	0.9463		80	7.6661	0.9830
	90	8.3672	0.7829		90	7.4662	0.8110
	100	8.1451	0.6422		100	7.3181	0.7462
30	10	10.5447	2.3948	210	10	9.6262	2.0233
	20	9.9596	2.0498		20	8.9812	1.5484
	30	9.6129	1.6851		30	8.6833	1.6439
	40	9.1511	1.4519		40	8.3000	1.5812
	50	9.1326	1.4305		50	8.2374	1.5650
	60	8.6311	1.0111		60	7.4231	1.2693
	70	8.7700	1.2245		70	7.7831	1.3201
	80	8.5761	1.0826		80	7.5425	1.1640
	90	8.3001	1.0984		90	7.2541	1.1126
	100	8.1092	1.0718		100	7.0531	0.9608
45	10	9.8744	2.3957	225	10	8.9373	1.9976
	20	9.2311	1.7149		20	8.2956	1.4442
	30	9.0481	1.6650		30	8.1636	1.4963
	40	8.5387	1.1588		40	7.7412	1.2010
	50	8.3741	1.4496		50	7.7188	1.4714
	60	8.6547	1.3639		60	7.4770	1.1934
	70	8.3362	1.2340		70	7.3487	1.2298
	80	8.0820	1.3067		80	7.1410	1.2905
	90	7.8533	1.2252		90	6.8703	1.2240
	100	7.5786	1.1344		100	6.6791	1.1621
60	10	9.0755	2.5092	240	10	7.8881	1.8668
	20	8.4351	2.0025		20	7.3432	1.4171
	30	7.9250	1.8385		30	6.8544	1.1838
	40	7.8246	1.9041		40	6.7833	1.2208
	50	7.2272	1.1859		50	6.3559	0.8483
	60	8.2981	1.8042		60	6.8582	1.1309
	70	7.3770	1.6112		70	6.3833	1.0642
	80	7.1431	1.4132		80	6.1620	1.0109
	90	6.8791	1.2334		90	5.9195	0.8986
	100	6.7181	0.9677		100	6.6900	0.7379
75	10	7.9356	2.1883	255	10	7.2477	1.9553
	20	7.4933	1.7968		20	6.9045	1.4087
	30	6.8131	1.4339		30	6.3656	1.2917
	40	6.3361	1.0453		40	6.1451	1.0536
	50	6.5859	1.1926		50	6.0632	0.9883
	60	6.5293	1.3320		60	6.1090	1.1380
	70	6.2540	1.1064		70	5.9224	0.9629
	80	6.0981	0.8921		80	5.7226	0.8309
	90	5.9603	0.7467		90	5.7850	0.8648
	100	5.8373	0.5905		100	5.4003	0.5677
90	10	7.0272	2.4874	270	10	6.8523	2.1377
	20	6.7210	1.8694		20	6.3523	1.6560

	30	6.3784	1.4929		30	6.0337	1.3998
	40	6.0293	1.1912		40	5.9224	1.3886
	50	6.1884	1.2206		50	5.8177	1.1995
	60	6.1190	1.2062		60	6.0111	1.3044
	70	5.9641	1.1177		70	5.8833	1.2923
	80	5.8982	0.9680		80	5.7481	1.2242
	90	5.8332	0.9337		90	5.8310	0.9231
	100	5.8276	0.8405		100	5.5914	0.9523
	10	7.8275	2.4935		10	7.0764	1.5386
	20	7.2524	1.7772		20	6.5345	1.1169
	30	6.7179	1.2794		30	6.1413	0.9798
	40	6.3534	1.0062		40	5.8853	1.0007
105	50	6.5030	1.2474	285	50	5.7866	0.9245
	60	6.4911	1.5241		60	6.1012	1.3789
	70	6.1771	1.3392		70	5.8737	1.2926
	80	5.9972	1.1066		80	5.6500	1.1515
	90	5.9050	1.0024		90	5.4772	1.0424
105	100	5.8414	0.8529	285	100	5.3685	0.9571
	10	9.1127	2.4071		10	8.5022	1.7660
	20	8.5513	1.9175		20	7.8511	1.3717
	30	8.2402	1.5978		30	7.5667	1.2339
	40	7.9977	1.4306		40	7.3211	1.0433
120	50	7.3614	1.0404	300	50	6.9833	1.1301
	60	7.8541	1.2019		60	7.1079	0.9066
	70	7.2572	1.0793		70	6.8333	0.9414
	80	7.0704	0.9557		80	6.6517	0.8883
	90	6.8619	0.8278		90	6.4512	0.8484
	100	6.6964	0.7785		100	6.3154	0.8254
	10	9.3165	2.0524		10	10.1736	2.5002
	20	8.5978	1.5624		20	9.4947	2.1335
	30	8.1356	1.3338		30	8.9945	1.7520
	40	7.8496	1.0122		40	8.6100	1.5135
135	50	7.4142	1.0034	315	50	8.1522	1.4301
	60	7.6961	1.3057		60	8.7262	1.5348
	70	7.3952	1.1764		70	8.3963	1.6146
	80	7.0922	1.1639		80	7.6686	1.3967
	90	6.9227	1.0501		90	7.4693	1.1613
	100	6.7641	0.9207		100	7.3590	1.1010
	10	10.5180	2.5185		10	9.8695	2.3056
	20	9.5954	1.9277		20	9.0412	1.6325
	30	8.9545	1.7049		30	8.3925	1.6217
	40	8.9364	1.4774		40	8.3692	1.3418
150	50	8.4334	1.2041	330	50	7.9014	1.2522
	60	8.8462	1.6082		60	8.0931	1.3041
	70	8.2161	1.3588		70	7.9430	1.1421
	80	8.0202	1.1037		80	7.6601	1.0313
	90	7.6638	1.0257		90	7.3525	1.0324
	100	7.4492	0.9130		100	7.1028	0.9392
	10	10.6543	2.2913		10	9.7433	2.0098
165	20	9.9955	1.6818	345	20	9.2146	1.6491
	30	9.5722	1.5881		30	8.8033	1.1898

	40	8.9070	1.6206		40	8.5143	1.2073
	50	8.6527	1.5085		50	7.8935	1.1648
	60	8.6762	1.6154		60	7.8888	1.0518
	70	8.4030	1.3793		70	7.7577	1.0386
	80	8.1164	1.2253		80	7.4773	0.9410
	90	7.9124	1.1049		90	7.1833	0.8261
	100	7.7224	0.9357		100	7.0093	0.7396

Table 2. JRC-CNNCVs of E_{JRC} in 24 different directions under 10 different sample sizes

Direction (°)	Size (cm)	E_{JRC}	Direction (°)	Size (cm)	E_{JRC}
	10	<[9.8233, 11.3490], 10.5861>		10	<[9.1289, 10.5635], 9.8462>
	20	<[9.1077, 10.2589], 9.6833>		20	<[9.3279, 10.5698], 9.9489>
	30	<[8.8129, 9.8143], 9.3136>		30	<[8.2076, 9.3679], 8.7877>
	40	<[8.3183, 9.4060], 9.0054>		40	<[8.0788, 9.2012], 8.6400>
0	50	<[8.4322, 9.5787], 8.8621>	180	50	<[7.7952, 8.8603], 8.3278>
	60	<[8.2928, 9.3715], 8.8322>		60	<[7.6219, 8.7128], 8.1673>
	70	<[8.1547, 9.2296], 8.6922>		70	<[7.4956, 8.4945], 7.9951>
	80	<[8.1064, 9.1075], 8.6070>		80	<[7.4591, 8.3570], 7.9080>
	90	<[8.1244, 9.0270], 8.5757>		90	<[7.4414, 8.2366], 7.8390>
	100	<[8.0419, 8.8948], 8.4684>		100	<[7.4804, 8.1882], 7.8343>
	10	<[9.9754, 11.4472], 10.7113>		10	<[9.0142, 10.5028], 9.7585>
	20	<[9.4157, 10.5813], 9.9985>		20	<[8.6896, 9.8636], 9.2766>
	30	<[8.8425, 9.9253], 9.3839>		30	<[8.1456, 9.2722], 8.7089>
	40	<[8.8721, 9.7305], 9.3013>		40	<[8.3509, 9.3277], 8.8393>
15	50	<[8.8445, 9.7083], 9.2764>	195	50	<[8.0389, 9.0834], 8.5611>
	60	<[8.5633, 9.4434], 9.0033>		60	<[7.6191, 8.6649], 8.1420>
	70	<[8.4500, 9.2360], 8.8430>		70	<[7.5291, 8.3754], 7.9523>
	80	<[8.2787, 8.9057], 8.5922>		80	<[7.3405, 7.9918], 7.6661>
	90	<[8.1078, 8.6266], 8.3672>		90	<[7.1975, 7.7349], 7.4662>
	100	<[7.9324, 8.3579], 8.1451>		100	<[7.0709, 7.5653], 7.3181>
	10	<[9.7513, 11.3380], 10.5447>		10	<[8.9559, 10.2965], 9.6262>
	20	<[9.2805, 10.6387], 9.9596>		20	<[8.4682, 9.4941], 8.9812>
	30	<[9.0547, 10.1712], 9.6129>		30	<[8.1387, 9.2280], 8.6833>
	40	<[8.6701, 9.6321], 9.1511>		40	<[7.7762, 8.8239], 8.3000>
30	50	<[8.6587, 9.6066], 9.1326>	210	50	<[7.7189, 8.7559], 8.2374>
	60	<[8.2961, 8.9661], 8.6311>		60	<[7.0026, 7.8436], 7.4231>
	70	<[8.3644, 9.1757], 8.7700>		70	<[7.3457, 8.2204], 7.7831>
	80	<[8.2175, 8.9348], 8.5761>		80	<[7.1569, 7.9281], 7.5425>
	90	<[7.9362, 8.6640], 8.3001>		90	<[6.8855, 7.6227], 7.2541>
	100	<[7.7541, 8.4643], 8.1092>		100	<[6.7348, 7.3714], 7.0531>
	10	<[9.0807, 10.6681], 9.8744>		10	<[8.2755, 9.5991], 8.9373>
	20	<[8.6630, 9.7993], 9.2311>		20	<[7.8172, 8.7741], 8.2956>
	30	<[8.4965, 9.5997], 9.0481>		30	<[7.6679, 8.6594], 8.1636>
	40	<[8.1548, 8.9227], 8.5387>		40	<[7.3433, 8.1391], 7.7412>
45	50	<[7.8939, 8.8544], 8.3741>	225	50	<[7.2313, 8.2063], 7.7188>
	60	<[8.2028, 9.1065], 8.6547>		60	<[7.0817, 7.8724], 7.4770>
	70	<[7.9274, 8.7450], 8.3362>		70	<[6.9412, 7.7561], 7.3487>
	80	<[7.6491, 8.5149], 8.0820>		80	<[6.7135, 7.5686], 7.1410>
	90	<[7.4474, 8.2592], 7.8533>		90	<[6.4648, 7.2758], 6.8703>

	100	<[7.2028, 7.9544], 7.5786>		100	<[6.2941, 7.0641], 6.6791>
	10	<[8.2442, 9.9068], 9.0755>		10	<[7.2697, 8.5066], 7.8881>
	20	<[7.7717, 9.0986], 8.4351>		20	<[6.8737, 7.8127], 7.3432>
	30	<[7.3159, 8.5341], 7.9250>		30	<[6.4622, 7.2466], 6.8544>
	40	<[7.1938, 8.4554], 7.8246>		40	<[6.3789, 7.1878], 6.7833>
60	50	<[6.8343, 7.6200], 7.2272>	240	50	<[6.0748, 6.6369], 6.3559>
	60	<[7.7004, 8.8958], 8.2981>		60	<[6.4835, 7.2329], 6.8582>
	70	<[6.8432, 7.9108], 7.3770>		70	<[6.0308, 6.7359], 6.3833>
	80	<[6.6749, 7.6113], 7.1431>		80	<[5.8271, 6.4969], 6.1620>
	90	<[6.4704, 7.2877], 6.8791>		90	<[5.6218, 6.2172], 5.9195>
	100	<[6.3975, 7.0386], 6.7181>		100	<[6.4456, 6.9345], 6.6900>
	10	<[7.2106, 8.6605], 7.9356>		10	<[6.5999, 7.8954], 7.2477>
	20	<[6.8980, 8.0885], 7.4933>		20	<[6.4378, 7.3712], 6.9045>
	30	<[6.3381, 7.2882], 6.8131>		30	<[5.9376, 6.7935], 6.3656>
	40	<[5.9898, 6.6824], 6.3361>		40	<[5.7960, 6.4941], 6.1451>
75	50	<[6.1908, 6.9810], 6.5859>	255	50	<[5.7358, 6.3907], 6.0632>
	60	<[6.0880, 6.9706], 6.5293>		60	<[5.7320, 6.4861], 6.1090>
	70	<[5.8875, 6.6206], 6.2540>		70	<[5.6034, 6.2414], 5.9224>
	80	<[5.8025, 6.3937], 6.0981>		80	<[5.4474, 5.9979], 5.7226>
	90	<[5.7129,6.2077], 5.9603>		90	<[5.4985, 6.0715], 5.7850>
	100	<[5.6417, 6.0330], 5.8373>		100	<[5.2122, 5.5884], 5.4003>
	10	<[6.2031, 7.8512], 7.0272>		10	<[6.1440, 7.5605], 6.8523>
	20	<[6.1017, 7.3404], 6.7210>		20	<[5.8037, 6.9009], 6.3523>
	30	<[5.8838, 6.8730], 6.3784>		30	<[5.5699, 6.4974], 6.0337>
	40	<[5.6347, 6.4239], 6.0293>		40	<[5.4623, 6.3824], 5.9224>
90	50	<[5.7840, 6.5928], 6.1884>	270	50	<[5.4203, 6.2151], 5.8177>
	60	<[5.7194, 6.5186], 6.1190>		60	<[5.5790, 6.4433], 6.0111>
	70	<[5.5938, 6.3344], 5.9641>		70	<[5.4552, 6.3115], 5.8833>
	80	<[5.5775, 6.2189], 5.8982>		80	<[5.3425, 6.1537], 5.7481>
	90	<[5.5238, 6.1425], 5.8332>		90	<[5.5252, 6.1369], 5.8310>
	100	<[5.5491, 6.1060], 5.8276>		100	<[5.2759, 5.9069], 5.5914>
	10	<[7.0014, 8.6536], 7.8275>		10	<[6.5667, 7.5862], 7.0764>
	20	<[6.6636, 7.8411], 7.2524>		20	<[6.1644, 6.9045], 6.5345>
	30	<[6.2941, 7.1418], 6.7179>		30	<[5.8166, 6.4659], 6.1413>
	40	<[6.0200, 6.6867], 6.3534>		40	<[5.5538, 6.2169], 5.8853>
105	50	<[6.0897, 6.9163], 6.5030>	285	50	<[5.4803, 6.0929], 5.7866>
	60	<[5.9862, 6.9960], 6.4911>		60	<[5.6444, 6.5580], 6.1012>
	70	<[5.7334, 6.6208], 6.1771>		70	<[5.4454, 6.3019], 5.8737>
	80	<[5.6306, 6.3638], 5.9972>		80	<[5.2685, 6.0315], 5.6500>
	90	<[5.5729, 6.2371], 5.9050>		90	<[5.1318, 5.8225], 5.4772>
	100	<[5.5588, 6.1239], 5.8414>		100	<[5.0514, 5.6855], 5.3685>
	10	<[8.3152, 9.9102], 9.1127>		10	<[7.9171, 9.0873], 8.5022>
	20	<[7.9160, 9.1865], 8.5513>		20	<[7.3966, 8.3055], 7.8511>
120	30	<[7.7108, 8.7695], 8.2402>	300	30	<[7.1579, 7.9755], 7.5667>
	40	<[7.5238, 8.4717], 7.9977>		40	<[6.9754, 7.6667], 7.3211>
	50	<[7.0167, 7.7061], 7.3614>		50	<[6.6089, 7.3577], 6.9833>
	60	<[7.4559, 8.2523], 7.8541>		60	<[6.8075, 7.4082], 7.1079>
	70	<[6.8996, 7.6148], 7.2572>		70	<[6.5214, 7.1451], 6.8333>
120	80	<[6.7538, 7.3871], 7.0704>	300	80	<[6.3574, 6.9460], 6.6517>
	90	<[6.5877, 7.1362], 6.8619>		90	<[6.1701, 6.7323], 6.4512>
	100	<[6.4384, 6.9543], 6.6964>		100	<[6.0419, 6.5889], 6.3154>

135	10	<[8.6366, 9.9965], 9.3165>	315	10	<[9.3453, 11.0019], 10.1736>
	20	<[8.0802, 9.1154], 8.5978>		20	<[8.7879, 10.2015], 9.4947>
	30	<[7.6937, 8.5775], 8.1356>		30	<[8.4140, 9.5749], 8.9945>
	40	<[7.5142, 8.1849], 7.8496>		40	<[8.1086, 9.1114], 8.6100>
	50	<[7.0817, 7.7466], 7.4142>		50	<[7.6784, 8.6260], 8.1522>
	60	<[7.2635, 8.1286], 7.6961>		60	<[8.2178, 9.2347], 8.7262>
	70	<[7.0055, 7.7850], 7.3952>		70	<[7.8614, 8.9312], 8.3963>
	80	<[6.7065, 7.4778], 7.0922>		80	<[7.2059, 8.1313], 7.6686>
	90	<[6.5748, 7.2706], 6.9227>		90	<[7.0846, 7.8541], 7.4693>
	100	<[6.4591, 7.0692], 6.7641>		100	<[6.9943, 7.7238], 7.3590>
150	10	<[9.6836, 11.3523], 10.5180>	330	10	<[9.1057, 10.6334], 9.8695>
	20	<[8.9568, 10.2341], 9.5954>		20	<[8.5003, 9.5820], 9.0412>
	30	<[8.3896, 9.5193], 8.9545>		30	<[7.8552, 8.9297], 8.3925>
	40	<[8.4469, 9.4258], 8.9364>		40	<[7.9246, 8.8137], 8.3692>
	50	<[8.0344, 8.8323], 8.4334>		50	<[7.4865, 8.3162], 7.9014>
	60	<[8.3134, 9.3790], 8.8462>		60	<[7.6610, 8.5251], 8.0931>
	70	<[7.7660, 8.6663], 8.2161>		70	<[7.5647, 8.3214], 7.9430>
	80	<[7.6545, 8.3858], 8.0202>		80	<[7.3184, 8.0018], 7.6601>
	90	<[7.3240, 8.0036], 7.6638>		90	<[7.0105, 7.6946], 7.3525>
	100	<[7.1468, 7.7517], 7.4492>		100	<[6.7917, 7.4140], 7.1028>
165	10	<[9.8952, 11.4134], 10.6543>	345	10	<[9.0775, 10.4091], 9.7433>
	20	<[9.4383, 10.5527], 9.9955>		20	<[8.6683, 9.7610], 9.2146>
	30	<[9.0461, 10.0983], 9.5722>		30	<[8.4091, 9.1975], 8.8033>
	40	<[8.3701, 9.4439], 8.9070>		40	<[8.1143, 8.9143], 8.5143>
	50	<[8.1530, 9.1525], 8.6527>		50	<[7.5076, 8.2794], 7.8935>
	60	<[8.1410, 9.2114], 8.6762>		60	<[7.5403, 8.2372], 7.8888>
	70	<[7.9461, 8.8600], 8.4030>		70	<[7.4136, 8.1018], 7.7577>
	80	<[7.7104, 8.5223], 8.1164>		80	<[7.1656, 7.7891], 7.4773>
	90	<[7.5463, 8.2784], 7.9124>		90	<[6.9096, 7.4570], 7.1833>
	100	<[7.4124, 8.0324], 7.7224>		100	<[6.7643, 7.2544], 7.0093>

As shown in Table 2, JRC-CNNCV reflects the mixed information of the confidence interval and the mean of the JRC values at the confidence level of 95%, which is different from the traditional expression methods of JRC-NNs. Furthermore, JRC-CNNCV reveals that 95% probability of the JRC data will fall within CNNs corresponding the confidence level of 95% and the mean magnitude of the JRC data. In this case, the confidence level can effectively guarantee the rationality and credibility of E_{JRC} from a probabilistic point of view. From a perspective of probabilistic estimation, the JRC-CNNCVs of E_{JRC} in Table 2 can contain 95% probability of the actual JRC values, but cannot contain 5% probability of them based on the probability estimation of the JRC values corresponding to different measurement directions and sample sizes.

To analyze the scale effect and anisotropy of the JRC values by the expression method of JRC-CNNCVs, we give Figures 1-3 and their analysis in detail.

Figure 1 shows the E_{JRC} values at different sizes in the measurement directions of 0°, 90°, 180°, and 270° from Table 2 and the average values of the corresponding JRC values in Table 1. As shown in Figure 1, the upper and lower bounds of JRC-CNNs and the JRC average values in the same measurement direction show a decreasing trend with the increase of the sample size, which is in line with the scale effect of the JRC values. At the same time, we can find that the standard deviation of the JRC values corresponding to each measurement direction generally shows a decreasing trend with the increase of the sample size. In Figure 2, taking the measurement direction of 15° as an example, the confidence intervals in E_{JRC} shrink with the increase of the sample size in the same direction, and then the JRC-CNNs and the JRC average values decrease with the increase of the sample size. This case also means that the uncertainty about the JRC values is diminishing with the increase of the sample size. In addition, we select the confidence intervals and the average values in E_{JRC} in the measurement directions from 0° to 345° under the sample sizes of 10 cm, 40 cm, 70 cm, and 100 cm to draw polar plots in Figure 3. As shown in Figure 3, the interval values of $[E^L, E^U]$ and the average values of v in different measurement directions under the same size are different, which reflect the anisotropy of the JRC values. Meanwhile, with increasing sample size, the upper and lower bounds of CNNs in different measurement directions under the same size are also close to each other, and the interval ranges of CNNs and the average values in E_{JRC} are decreasing, which indicates the scale effect of the anisotropy of the JRC values. The above conclusions show that the JRC values expressed by JRC-CNNCVs can also reflect indeterminate and incomplete information contained in the anisotropy of the JRC values. Therefore, it is obvious that the expression and analysis method using JRC-CNNCVs proposed in this study can effectively reveal the scale effect and anisotropy of the JRC values, then the proposed method is obviously superior to the existing methods regarding their rationality and credibility in the application scenarios of small-scale sample data.

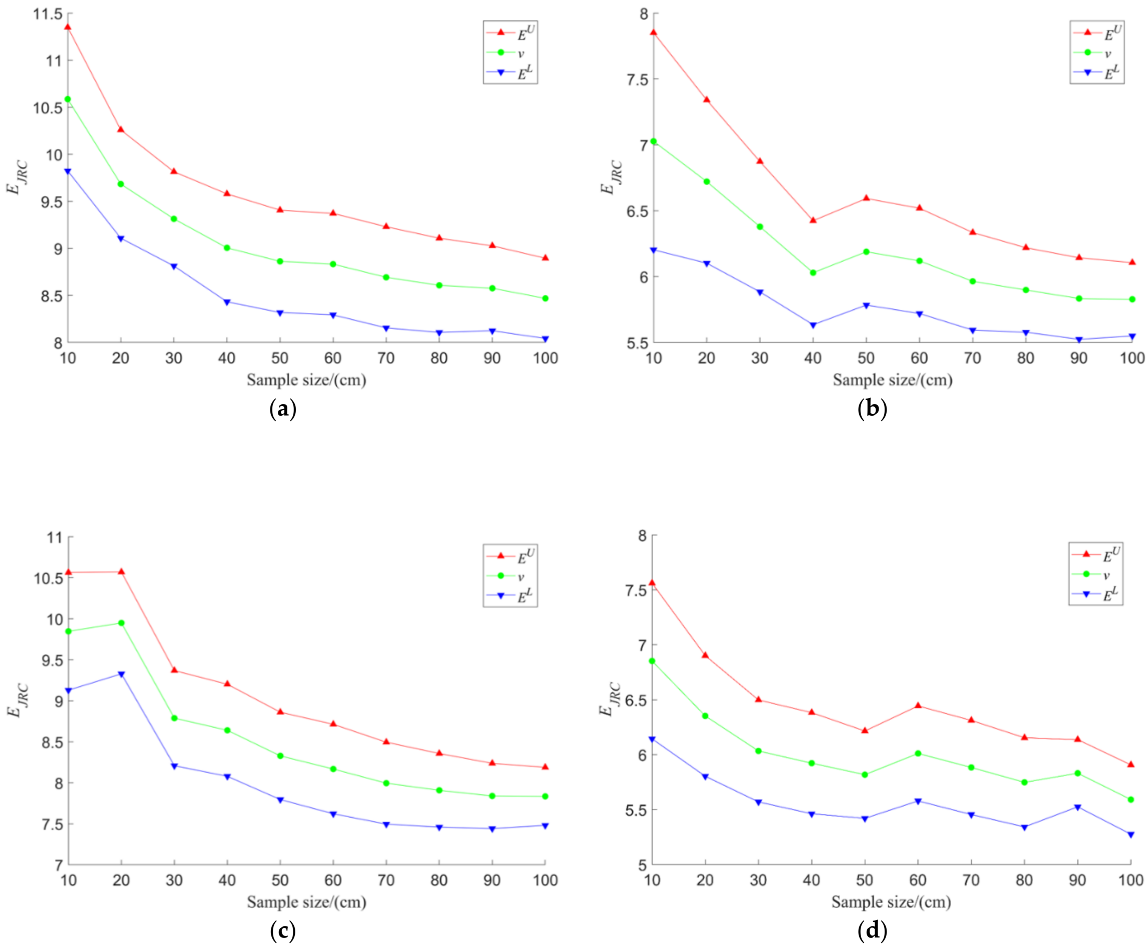

Figure 1. (**a**) E_{JRC} (JRC-CNNCVs) corresponding to JRC values at different sizes in the 0° direction; (**b**) E_{JRC} (JRC-CNNCVs) corresponding to the JRC values at different sizes in the 90° direction; (**c**) E_{JRC} (JRC-CNNCVs) corresponding to the JRC values at different sizes in the 180° direction; (**d**) E_{JRC} (JRC-CNNCVs) corresponding to the JRC values at different sizes in the 270° direction.

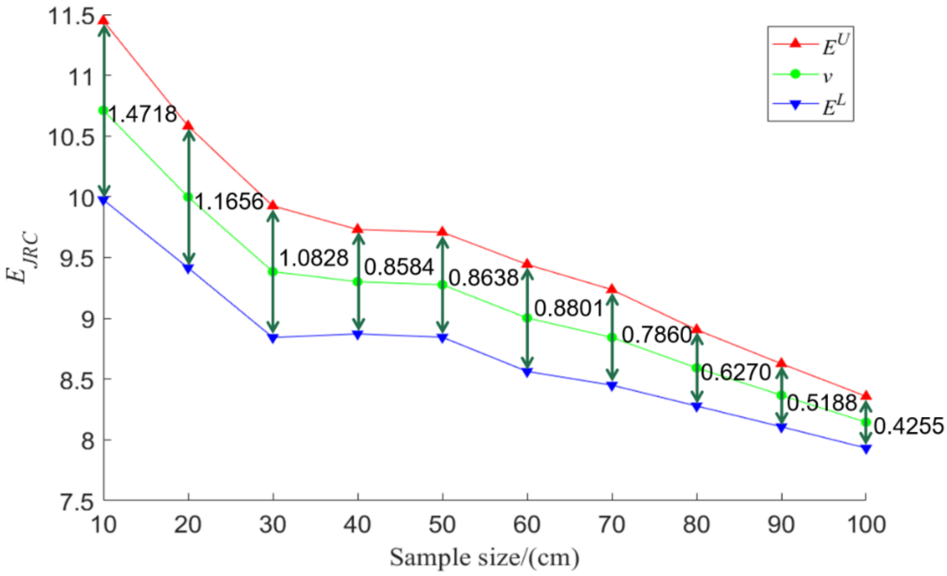

Figure 2. E_{JRC} (JRC-CNNCVs) corresponding to the JRC values of different sizes in the 15° direction

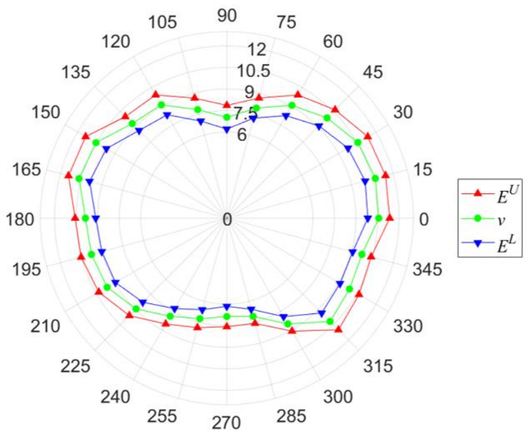

(**a**)

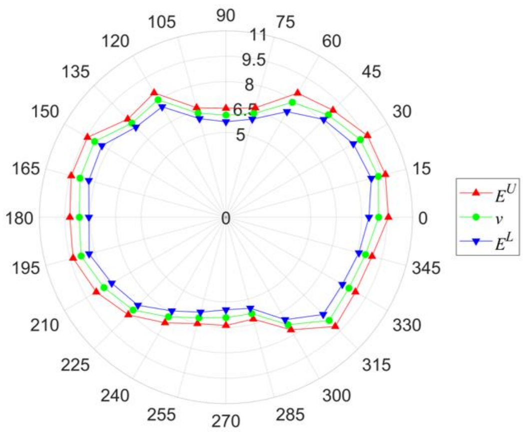

(**b**)

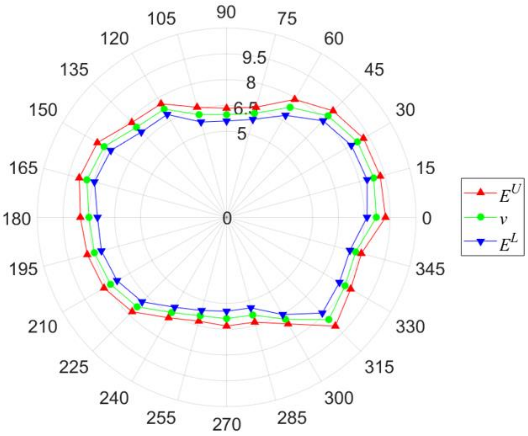

(**c**)

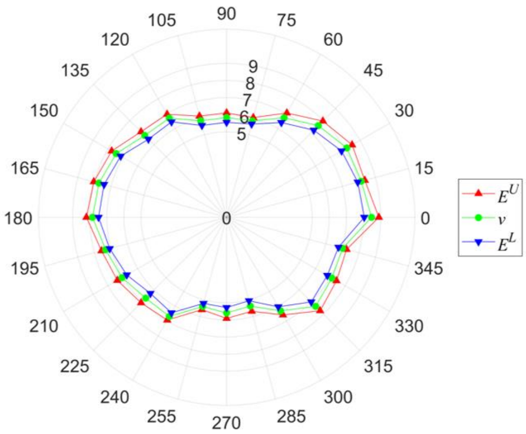

(**d**)

Figure 3. (**a**) E_{JRC} (JRC-CNNCVs) corresponding to the JRC values of different measurement directions under 10 cm sample size; (**b**) E_{JRC} (JRC-CNNCVs) corresponding to the JRC values of different measurement directions under 40 cm sample size; (**c**) E_{JRC} (JRC-CNNCVs) corresponding to the JRC values of different measurement directions under 70 cm sample size; (**d**) E_{JRC} (JRC-CNNCVs) corresponding to the JRC values of different measurement directions under 100 cm sample size

4. Conclusions

Since it is difficult to usually obtain enough large-scale JRC sample data from rock mass joint surfaces due to the limitation of the measurement environment, measurement technology, and other factors, there exists some indeterminate and incomplete information in small-scale JRC sample data. In this case, the existing representation and analysis methods of JRC sample data almost all lack the measures of confidence levels in sample data analysis. Then, the JRC-CNNCV expression obtained from the limited/small-scale JRC sample data can effectively solve the above problems and ensure that the JRC values can fall within CNN with a certain confidence level. Unlike classical statistics which takes the JRC values as crisp values, JRC-CNNCV transformed from the JRC values is composed of the confidence interval and the average value, so the uncertainty and incompleteness contained in the JRC values can be fully reflected by the probabilistic estimation within a confidence interval. As the extension and improvement of the existing JRC-NN expression methods for JRC values, the JRC-CNNCV expression method can effectively ensure the reliability of the small-scale sample data so as to lessen the loss of useful information and simplify the analysis process. In addition, through the expression and analysis method using JRC-CNNCVs for the JRC values of an actual case, this study also revealed the scale effect and anisotropy of the JRC values so as to further verify the effectiveness and convenience of the proposed expression and analysis method. It is clear that the proposed expression and analysis method can further enhance the credibility of the analysis results on the JRC characteristics (the scale effect and anisotropy of the JRC values) from a probabilistic point of view. In the future, CNNCVs combined with other analysis methods will present more in-depth analysis of the scale effect and anisotropy of the JRC values, and the CNNCV expression and analysis method will be further extended to engineering or experiment data processing.

Funding: This research received no external funding.

Conflicts of Interest: The authors declare no conflict of interest.

References

1. Barton, N. Review of a new shear-strength criterion for rock joints. *Engineering Geology* **1973**, 7, 287–332.
2. Tse, R. Estimating joint roughness coefficients. *International Journal of Rock Mechanics & Mining Sciences & Geomechanics Abstracts* **1979**, 16, 303–307.
3. Zhang, G.; Karakus, M.; Tang, H.; Ge, Y.; Zhang, L. A new method estimating the 2D joint roughness coefficient for discontinuity surfaces in rock masses. *International Journal of Rock Mechanics and Mining Sciences* **2014**, 72, 191–198.
4. Barton, N.; Bandis, S. *Effects of block size on the shear behavior of jointed rock*. In: The 23rd US symposium on rock mechanics (USRMS), OnePetro **1982**.
5. Barton, N.; Bandis, S. *Review of predictive capabilities of JRC-JCS model in engineering practice*. Rock Joints, Balkema, Rotterdam, **1990**, pp. 603–610.
6. Du, S.G.; Yu, C.; Liangben, F. Maethematical expression of JRC modified straight edge. *Chinese Journal of Geophysics* **1996**, 4, 36–43.
7. Hu, X.; Du, S.G. Concise formula of Barton's straight edge method for joint roughness coefficient. *Chinese Journal of Geophysics* **2008**, 16(2), 196–200.
8. Lee, Y.H.; Carr, J.R.; Barr, D.J.; Haas, C.J. The fractal dimension as a measure of the roughness of rock discontinuity profiles. *International Journal of Rock Mechanics and Mining Science & Geomechanics Abstracts* **1990**, 27, 453–464.

9. Xie, H.; Wang, J.A.; Xie, W.H. Fractal effects of surface roughness on the mechanical behavior of rock joints. *Chaos, Solitons & Fractals* **1997**, 8, 221–252.
10. Xie, H.; Wang, J.A.; Kwaśniewski, M. Multifractal characterization of rock fracture surfaces. *International Journal of Rock Mechanics and Mining Sciences* **1999**, 36, 19–27.
11. Xie, H.; Wang, J.A.; Stein, E. Direct fractal measurement and multifractal properties of fracture surfaces. *Physics letters A* **1998**, 242, 41–50.
12. Bandis, S.; Lumsden, A.; Barton, N. *Experimental studies of scale effects on the shear behaviour of rock joints*. In: International journal of rock mechanics and mining sciences & geomechanics abstracts. Elsevier **1981**, pp. 1–21.
13. Barton, N.; Choubey, V. The shear strength of rock joints in theory and practice. *Rock mechanics* **1977**, 10, 1–54.
14. Odling, N. Natural fracture profiles, fractal dimension and joint roughness coefficients. *Rock mechanics and rock engineering* **1994**, 27, 135–153.
15. Du, S.G.; Fan, L.B. The statistical estimation of rock joint roughness coefficient. *Chinese Journal of Geophysics-Chinese Edition* **1999**, 42(4), 577–580.
16. Aydan, Ö.; Shimizu, Y.; Kawamoto, T. The anisotropy of surface morphology characteristics of rock discontinuities. *Rock mechanics and rock engineering* **1996**, 29, 47–59.
17. Belem, T.; Homand-Etienne, F.; Souley, M. Quantitative parameters for rock joint surface roughness. *Rock mechanics and rock engineering* **2000**, 33, 217–242.
18. Du, S.G. *Engineering behavior of discontinuities in rock mass*. Seismological Press **1999**.
19. Du, S.G.; Tang, H. A study on the anisotropy of joint roughness coefficient in rock mass. *Journal of Engineering Geology* **1993**, 1, 32–42.
20. Zhang, G.; Bao, H.; Lan, H.; Yan, C.; Tao, Y. Research on the relationship between joint roughness coefficient and sampling precision of structural plane. *Journal of Engineering Geology* **2018**, 26, 1336–1341.
21. Huang, M.; Xia, C.; Sha, P.; Ma, C.; Du, S. Correlation between the joint roughness coefficient and rock joint statistical parameters at different sampling intervals. *Advances in Civil Engineering* **2019**, 2019, 1643842.
22. Smarandache, F. *Neutrosophy: neutrosophic probability, set and logic*. American Research Press, Rehoboth, USA **1998**.
23. Smarandache, F. *Introduction to neutrosophic measure, neutrosophic integral, and neutrosophic probability*. Sitech & Education Publishing, Craiova, USA **2013**.
24. Smarandache, F. *Introduction to Neutrosophic Statistics*. Sitech & Education Publishing, Craiova, USA **2014**.
25. Ye, J. Bidirectional projection method for multiple attribute group decision making with neutrosophic numbers. *Neural Computing and Applications* **2015**, 5, 1021–1029.
26. Ye, J. Multiple-attribute group decision-making method under a neutrosophic number environment. *Journal of Intelligent Systems* **2016**, 25, 377–386.
27. Ye, J. Fault diagnoses of steam turbine using the exponential similarity measure of neutrosophic numbers. *Journal of Intelligent & Fuzzy Systems* **2016**, 30, 1927–1934.
28. Zhang, M.; Liu, P.; Shi, L. An extended multiple attribute group decision-making TODIM method based on the neutrosophic numbers. *Journal of Intelligent & Fuzzy Systems* **2016**, 30, 1773–1781.
29. Liu, P.; Liu, X. The neutrosophic number generalized weighted power averaging operator and its application in multiple attribute group decision making. *International Journal of Machine Learning and Cybernetics* **2018**, 9, 347–358.
30. Aslam, M.; Khan, N.; Khan, M.Z. Monitoring the variability in the process using neutrosophic statistical interval method. *Symmetry* **2018**, 10, 562.
31. Santillán, M.A.; Cacpata, C.W.A.; Bosquez, R.J.D. Opportunities for software testing using neutrosophic numbers. *Neutrosophic Sets and Systems* **2020**, 37, 267–276.
32. Maiti, I.; Mandal, T.; Pramanik, S. Neutrosophic goal programming strategy for multi-level multi-objective linear programming problem. *Journal of Ambient Intelligence and Humanized Computing* **2020**, 11, 3175–3186.
33. Liu, P.; Chu, Y.; Li, Y.; Chen, Y. Some generalized neutrosophic number Hamacher aggregation operators and their application to group decision making. *International Journal of fuzzy systems* **2014**, 16(2), 242–255.
34. Yong, R.; Gu, L.Y.; Ye, J.; Du, S.G.; Huang, M. Neutrosophic function with NNs for analyzing and expressing anisotropy characteristic and scale effect of joint surface roughness. *Mathematical Problems in Engineering* **2019**, 2019, 8718936.

35. Chen, J.Q.; Ye, J.; Du, S.G. Scale effect and anisotropy analyzed for neutrosophic numbers of rock joint roughness coefficient based on neutrosophic statistics. *Symmetry* **2017**, 9(10), 208.
36. Aslam, M. A new method to analyze rock joint roughness coefficient based on neutrosophic statistics. *Measurement* **2019**, 146, 65–71.
37. Aslam, M.; Bantan, R.A.; Khan, N. Design of tests for mean and variance under complexity-an application to rock measurement data. *Measurement* **2021**, 177, 109312.
38. Chen, J.Q.; Ye, J.; Du, S.G.; Yong, R. Expressions of rock joint roughness coefficient using neutrosophic interval statistical numbers. *Symmetry* **2017**, 9(7), 123.
39. Zhang, S.; Ye, J. Group decision-making model using the exponential similarity measure of confidence neutrosophic number cubic sets in a fuzzy multi-valued circumstance. *Neutrosophic Sets and Systems* **2023**, 53, 130–138.
40. Lv, G.; Du, S.G.; Ye, J. Confidence neutrosophic number linear programming methods based on probability distributions and their applications in production planning problems. *Mathematical Problems in Engineering* **2022**, 2022, 5243797.
41. Bao, H.; Zhang, G.; Lan, H.; Yan, C.; Xu, J.; Xu, W. Geometrical heterogeneity of the joint roughness coefficient revealed by 3D laser scanning. *Engineering Geology* **2020**, 265, 105415.
42. Beer, A.; Stead, D.; Coggan, J. Technical Note Estimation of the Joint Roughness Coefficient (JRC) by Visual Comparison. *Rock Mechanics and Rock Engineering* **2002**, 1, 65–74.
43. Kim, D.H.; Poropat, G.V.; Gratchev, I.; Balasubramaniam, A. Improvement of photogrammetric JRC data distributions based on parabolic error models. *International Journal of Rock Mechanics and Mining Sciences* **2015**, 80, 19–30.
44. Luo, S.; Zhao, Z.; Peng, H.; Pu, H. The role of fracture surface roughness in macroscopic fluid flow and heat transfer in fractured rocks. *International Journal of Rock Mechanics and Mining Sciences* **2016**, 87, 29–38.

Received: August 6, 2022. Accepted: January 7, 2023